

Transient light-induced absorption in periodically poled lithium niobate: Small polaron hopping in the presence of a spatially modulated defect concentration

B. Schoke, M. Imlau,* H. Brüning, and C. Merschjann
Fachbereich Physik, Universität Osnabrück, Osnabrück, Germany
and Helmholtz-Zentrum Berlin für Materialien und Energie GmbH, Berlin, Germany

G. Corradi and K. Polgár
Research Institute for Solid State Physics and Optics, Hungarian Academy of Sciences, Budapest, Hungary

I. I. Naumova
Physics Department, Moscow State University, Moscow, Russia

(Received 11 March 2010; published 7 April 2010)

The study of the transient light-induced absorption in thermally reduced, periodically poled lithium niobate doped with Y uncovers the simultaneous action of the $\text{Nb}_{\text{Li}}^{4+}:\text{Nb}_{\text{Nb}}^{4+}$ bipolaron and O^- hole polaron relaxation in the blue and near-infrared spectral range. The findings can be comprehensively explained taking into account a periodic, spatial modulation of the $\text{Nb}_{\text{Li}}^{5+}$ antisite defect distribution, which results in a modulation of both concentrations and relaxation lifetimes of optically excited, small bound electron and hole polarons and bipolarons.

DOI: [10.1103/PhysRevB.81.132301](https://doi.org/10.1103/PhysRevB.81.132301)

PACS number(s): 71.38.Ht, 71.38.Mx, 77.84.Ek

I. INTRODUCTION

Transient light-induced absorption of oxide materials such as KNbO_3 (Refs. 1 and 2) and LiNbO_3 (Ref. 3) allows to probe small polarons bound to defects thus clarifying the related hopping transport processes and relaxation kinetics. A key point of interest is the understanding and control of polaron hopping in crystalline dielectric environment with disordered or clustered defect distribution, also motivated by the essential role of small bound polarons in the field of optical damage,¹ radiation or light-induced absorption,⁴ and photorefractivity.^{1,3} Extending these studies to periodically poled lithium niobate (PPLN) widely used for quasiphase matching applications is an important step into this direction.

We show time-resolved measurements of the light-induced absorption $\alpha_i(t)$ in the blue and near-infrared spectral range upon illumination with intense green laser pulses, which uncover the simultaneous action of the $\text{Nb}_{\text{Li}}^{4+}:\text{Nb}_{\text{Nb}}^{4+}$ bipolaron and O^- hole polaron relaxation. The findings are explained considering the periodic, spatial modulation of $\text{Nb}_{\text{Li}}^{4+}:\text{Nb}_{\text{Nb}}^{4+}$ and $\text{Nb}_{\text{Li}}^{5+}$ antisite defects: optical excitation in the presence of this intrinsic defect modulation results in a modulation of both concentrations and relaxation lifetimes of optically excited, small bound electron and hole polarons. The overall signal represents the superposition of transient light-induced absorptions from individual regions with different defect structure. Under these assumptions the observed multicomponent decay spectra can be understood without postulating further deep or shallow traps.

II. EXPERIMENTAL DETAILS

The PPLN sample was cut from a boule of bulk periodically poled $\text{LiNbO}_3:\text{Y}$ grown by Naumova from a closely congruent composition using the *off-center Czochralski* technique. The ferroelectric domain structure of period

$\Lambda \approx 24 \mu\text{m}$ is a result of rotation-induced striations and Y doping (1 wt % Y_2O_3 in the melt).⁵ A single-domain sample of Y-doped LiNbO_3 (1 wt % Y_2O_3 in the melt, grown by Polgár) and a nominally undoped LiNbO_3 wafer ($c_{\text{Fe}} < 5$ ppm, purchased from Crystal Technology, Inc.) served for reference. All crystals were thermally reduced by vacuum annealing ($p < 10^{-4}$ mbar) at elevated temperatures for a duration of 6 h. Hence, the properties of small bound $\text{Nb}_{\text{Li}}^{4+}$ polarons ($\lambda_{\text{abs}} = 760$ nm, 1.6 eV), $\text{Nb}_{\text{Li}}^{4+}:\text{Nb}_{\text{Nb}}^{4+}$ bipolarons and O^- hole polarons (both at 500 nm, 2.5 eV) (Refs. 6 and 7) could be studied. The reduction temperatures T_{R} were adjusted to obtain a similar degree of reduction represented by a steady-state absorption of $\alpha_{500} \sim 400 \text{ m}^{-1}$ at $\lambda = 500$ nm (cf. Table I).⁸ The pump beam in the setup for time-resolved pump-multiprobe spectroscopy (cf. Ref. 8) was applied perpendicularly to both the crystal c axis and the wave vector of the domain structure. Spectra were collected subsequent to single pulses of a frequency-doubled YAG:Nd laser ($\lambda = 532$ nm, pulse width $\tau_{\text{p}} \sim 8$ ns).

III. EXPERIMENTAL RESULTS

Figure 1 highlights the temporal evolution of the light-induced absorption. The data are normalized to the maxi-

TABLE I. Y_2O_3 concentrations in the melt, reduction temperatures T_{R} , steady-state absorption α_{500} at $\lambda = 500$ nm, and thicknesses d of the studied samples.

| Sample | $c(\text{Y}_2\text{O}_3)$ | T_{R} (K) | α_{500} (m^{-1}) | d (mm) |
|---------------------------|---------------------------|-----------------------|---------------------------------------|-----------------|
| LiNbO_3 | | 920 | 410 ± 10 | 2.87 ± 0.01 |
| $\text{LiNbO}_3:\text{Y}$ | 1 wt % | 770 | 395 ± 10 | 0.85 ± 0.01 |
| PPLN:Y | 1 wt % | 970 | 400 ± 10 | 2.20 ± 0.01 |

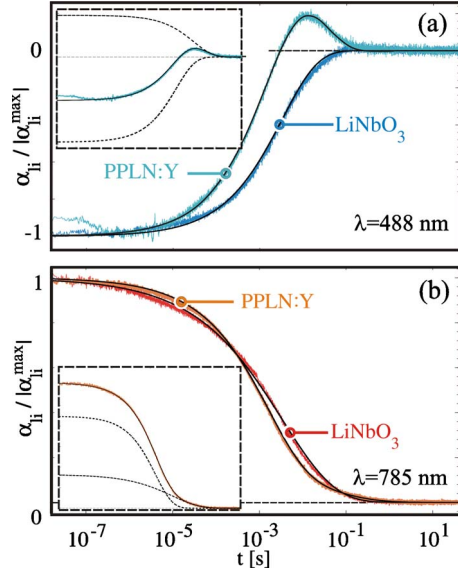


FIG. 1. (Color online) Temporal behavior of the light-induced absorption in reduced PPLN:Y and reduced single-domain nominally pure lithium niobate probed at (a) $\lambda=488$ nm and (b) $\lambda=785$ nm ($I_p=800$ GW/m²). Insets: complete fits for PPLN:Y according to Eq. (1) (solid line) and its single components (dashed lines).

imum starting amplitude $|\alpha_{ii}^{\max}|$ and are presented for a pulse intensity of $I_p=800$ GW/m² with probe light ($I < 1.6$ kW/m²) at (a) 488 nm and (b) 785 nm close to the absorption maxima of the small bound polarons. The measurements were performed at room temperature and with ordinary pump and probe light polarization ($\mathbf{e}_p \perp \mathbf{c}$ axis) yielding the maximum signal amplitude (cf. Ref. 9).

Experimental data for single-domain, nominally pure LiNbO₃ are included for reference. For the PPLN:Y sample a transient transparency at 488 nm initially induced by the pump pulse changes to a transient absorption at 1 ms prior to its decay ($t > 0.1$ s). Obviously, it is a result of two superimposed decay components with different time constants and opposite sign in their amplitudes. The comparison with the single-domain, nominally pure sample, where a single relaxation component gives an adequate description, highlights a further particularity of the PPLN:Y signal at 785 nm [Fig. 1(b)]: here, the decay shape of the light-induced absorption is altered with respect to the single-domain sample resulting in an intersection point of the two spectra at $t_{ip}=0.3$ ms.

The PPLN:Y signal is analyzed by fitting the data set with the sum of two stretched exponential functions (solid line in Fig. 1), which are widely established for the description of hopping-transport related relaxation processes of small polarons in oxide materials,^{4,10-12}

$$\alpha_{ii}(t) = \alpha_{ii}^{(1)} \exp\left[\left(-\frac{t}{\tau_1}\right)^{\beta_1}\right] + \alpha_{ii}^{(2)} \exp\left[\left(-\frac{t}{\tau_2}\right)^{\beta_2}\right]. \quad (1)$$

Here, $\alpha_{ii}^{(1,2)}$ denote the amplitudes, $\tau_{1,2}$ the relaxation times, and $\beta_{1,2}$ the stretching factors. The complete fit and its two components (dashed lines) are plotted separately in the insets of Fig. 1. Fitting parameters are given in Table II together

TABLE II. Parameters obtained from fits of $\alpha_{ii}(t)$ by stretched exponential functions, see Fig. 1 and Eq. (1).

| Sample | α_{ii} (m ⁻¹) | τ (ms) | β |
|-----------------------|-------------------------------------|----------------|-----------------|
| $\lambda=488$ nm | | | |
| LiNbO ₃ | (-87 ± 10) | 3.6 ± 0.5 | 0.52 ± 0.05 |
| LiNbO ₃ :Y | (-81 ± 10) | 8.2 ± 0.7 | 0.55 ± 0.05 |
| PPLN:Y | | | |
| Component (1) | (-122 ± 10) | 1.8 ± 0.7 | 0.53 ± 0.07 |
| Component (2) | (73 ± 10) | 10 ± 2 | 0.47 ± 0.07 |
| $\lambda=785$ nm | | | |
| LiNbO ₃ | (250 ± 15) | 3.3 ± 0.5 | 0.36 ± 0.05 |
| LiNbO ₃ :Y | (231 ± 10) | 7.7 ± 0.7 | 0.33 ± 0.05 |
| PPLN:Y | | | |
| Component (1) | (216 ± 15) | 1.7 ± 0.5 | 0.51 ± 0.05 |
| Component (2) | (91 ± 10) | 9 ± 2 | 0.30 ± 0.07 |

with the results of fitting single stretched exponential functions to the data set of the single-domain samples. We note that experimental data for the single-domain, Y-doped sample (omitted in Fig. 1 for reasons of clarity) revealed analogous behavior as obtained for the undoped sample, but with a significantly longer decay time.

IV. DISCUSSION

The characteristic feature of the PPLN:Y sample is the periodic ferroelectric domain structure induced by Y-doping and off-center Czochralski growth. Following Ref. 5, the Y concentration shows a saw-tooth-shaped, spatially periodic distribution over the crystal length where the concentration extrema are slightly displaced relative to the domain walls. It is therefore inevitable to first clarify the influence of homogeneous Y doping on the intrinsic defect structure and, in particular, on the polaron formation and relaxation properties. Our study on a thermally reduced, single-domain sample of Y-doped LiNbO₃ revealed an increase in the relaxation time τ by about 4 ms due to Y doping, independent of the probe wavelength (cf. Table II), while leaving the stretching factors β unaffected. This increase in the carrier relaxation time can be explained if we assume that the concentration of Nb_{Li}⁵⁺ is reduced by the incorporation of Y on Li sites. In this case, the recombination probability decreases due to the increased interdefect distances analogously to Mg-doped and near-stoichiometric lithium niobate in the model of a stoichiometry-dependent recombination process.^{4,13} In fact, a saw-tooth-shaped modulation of Y_{Li} in the PPLN:Y sample thus implies a spatial concentration distribution of Nb_{Li}⁵⁺, i.e., of stoichiometry, with inverse shape: maxima of $c_{\text{Nb}_{\text{Li}}}$ coincide with minima of $c_{\text{Y}_{\text{Li}}}$ and vice versa. Consequently, as bipolarons may be formed only at Nb_{Li} antisites, we expect a spatial modulation of bipolarons as well, which is in phase with the $c_{\text{Nb}_{\text{Li}}}$ modulation in the thermally reduced PPLN:Y sample. This expectation is verified by scanning the steady-

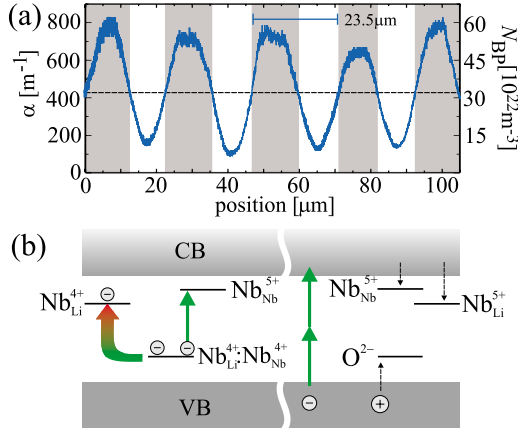


FIG. 2. (Color online) (a) Spatial modulation of the absorption at $\lambda=488$ nm and bipolaron concentration along the direction of the domain grating vector. (b) Model for polaron excitation in thermally reduced lithium niobate.

state absorption along the direction of the domain wave vector with probe light at 488 nm as shown in Fig. 2(a). The study was performed by homogeneous exposure of the PPLN crystal and detection of the transmission with a Si-PIN diode having an aperture of $d=5$ μm . It yields an average spatial frequency of $\Lambda_\alpha=(23.5 \pm 0.7)$ μm in coincidence with the domain period and an average steady-state absorption of 415 m^{-1} . The maximum up to 800 m^{-1} can be compared with the degree of reduction of $\alpha_{500}=760$ m^{-1} obtained for single domain lithium niobate at $T_R=970$ K.⁸ According to Ref. 14, the respective bipolaron concentrations can be determined using the absorption cross section $\sigma_{BP}^{488\text{ nm}}=(14 \pm 2) \times 10^{-22}$ m^2 . For simplicity, in what follows we consider the PPLN:Y sample as a stack of 12 - μm -wide lithium niobate layers with alternating bipolaron concentration as suggested by the gray shaded areas in Fig. 2(a). We note, that these areas should not be mixed up with the phase-shifted domain structure.

The generation and recombination scheme of small bound polarons can be described within each layer in accordance with the processes in reduced single-domain samples schematically depicted in Fig. 2(b):^{8,15} the light pulse at 532 nm causes the optical dissociation of $\text{Nb}_{\text{Li}}^{4+}:\text{Nb}_{\text{Nb}}^{4+}$ bipolarons, thus forming small free $\text{Nb}_{\text{Nb}}^{4+}$ and small bound $\text{Nb}_{\text{Li}}^{4+}$ polarons. This process is characterized by a *decrease* in the bipolaron absorption centered at 500 nm and an increase of free and bound polaron bands in the near-infrared spectral range centered at 1250 and 760 nm.⁶ At the same time, the light pulse generates O^- hole as well as free $\text{Nb}_{\text{Nb}}^{4+}$ and bound $\text{Nb}_{\text{Li}}^{4+}$ polarons via two-photon interband excitation. While this process also increases the $\text{Nb}_{\text{Nb}}^{4+}$ and $\text{Nb}_{\text{Li}}^{4+}$ near-infrared absorption bands, it yields a strong *increase* in the absorption at 500 nm related to hole polarons.⁷

In layers with a large bipolaron concentration, the optical gating of bipolarons will be efficient due to the pronounced steady-state absorption at the pump wavelength while the two-photon process generating O^- hole polarons will be suppressed due to the damping of the pump beam which reduces the probability for two-photon excitation processes. The result is a light-induced transparency in the blue spectral range.

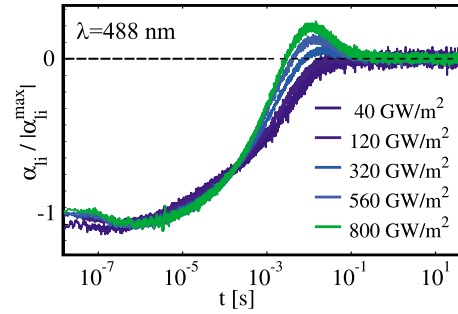


FIG. 3. (Color online) Temporal evolution of the light-induced absorption in reduced PPLN:Y depending on the pump intensity I_p for the probe wavelength $\lambda=488$ nm.

Layers with a lower bipolaron concentration lead to a significant contribution of the two-photon interband process yielding a high concentration of hole, free and bound polarons. A light-induced absorption will appear at 500 nm, also because the $\text{Nb}_{\text{Li}}^{4+}:\text{Nb}_{\text{Nb}}^{4+}$ concentration is low. We have to consider both cases for the starting value of the light-induced absorption in our PPLN:Y sample. Here, the pronounced light-induced transparency points to a dominating contribution of one-photon dissociations of bipolarons in the layers with large bipolaron concentration.

The change in the light-induced transparency to a light-induced absorption at about 1 ms indicates a significant difference in the respective lifetimes related to $\text{Nb}_{\text{Li}}^{4+}:\text{Nb}_{\text{Nb}}^{4+}$ recombination and O^- relaxation. Bipolaron recombination is determined by the interaction of small free and bound polarons; as the mobility of $\text{Nb}_{\text{Nb}}^{4+}$ is comparably large, the probability for $\text{Nb}_{\text{Nb}}^{4+}-\text{Nb}_{\text{Li}}^{4+}$ recombination increases with the number of antisite defect centers. Hence, the lifetime of $\text{Nb}_{\text{Li}}^{4+}:\text{Nb}_{\text{Nb}}^{4+}$ recombination is short in lithium niobate with a congruent composition. O^- relaxation is determined by the interaction of $\text{Nb}_{\text{Li}}^{4+}$ and O^- , so that the hole polaron lifetime increases with improving stoichiometry.

The key in understanding the behavior of the light-induced absorption are the different contributions from differently reduced layers to the overall signal: layers with a strong degree of reduction contribute mainly by the bipolaron behavior, i.e., by a light-induced transparency in the blue spectral range and a short recombination time due to a high antisite concentration in such layers. Layers with a small degree of reduction account for hole polaron properties, i.e., a light-induced absorption in the blue spectral range and a comparably long lifetime due to a near-stoichiometric composition. Hence, the deconvolution of the signal in two components according to the inset of Fig. 1(a) essentially indicates the respective contributions of bipolaron recombination and hole polaron relaxation to the overall signal.

The validity of our explanation is supported by studying the transient signal as a function of the pump intensity as depicted in Fig. 3. The intensity dependence displays the competition in polaron formation via one photon, i.e., optical dissociation of bipolarons, and two-photon processes, i.e., formation of hole polarons. The probability of two-photon processes strongly decreases with decreasing pump intensity, so that the contribution of the second component, related to O^- formation and relaxation, vanishes. As a result, the tran-

sient signal at low pump intensities reflects the dissociation and recombination of $\text{Nb}_{\text{Li}}^{4+}:\text{Nb}_{\text{Nb}}^{4+}$, only.

The results depicted in Fig. 1(b) can be explained in the frame of our simple model straightforwardly: at 785 nm, the number density of $\text{Nb}_{\text{Li}}^{5+}$ antisites dominates the absorption, i.e., again both O^- and $\text{Nb}_{\text{Li}}^{4+}:\text{Nb}_{\text{Nb}}^{4+}$ relaxation processes are probed simultaneously, but here with contributions of the same sign. Consequently, and since adequate fitting with a single stretched exponential function fails for the PPLN:Y sample, the transient decay must be fitted with the sum of two stretched exponential functions according to Eq. (1), as well. The respective fitting procedure at 785 nm reveals time constants nearly identical to those found for 488 nm (see Table II). The changes in the decay shape reflected in Fig. 1(b) hence originate from changed recombination properties in the PPLN:Y sample in comparison to the single-domain sample.

Obviously, our simple model of layers with different degree of stoichiometry and reduction is able to explain the transient light-induced absorption in PPLN:Y comprehensively, this reveals several consequences: (1) the lifetime of small polaron recombination reflected by the transient absorption/transparency is predominantly determined by the $\text{Nb}_{\text{Li}}^{5+}$ density. (An influence from the phase-shifted domain structure can be neglected.) (2) Population and depopulation dynamics between different deep and shallow traps⁹ can be excluded in the explanation of the observed multicomponent decay spectra. (3) Initial and final sites of a three-dimensional random walk of small polarons via hopping

must be predominantly located within the same PPLN layer. (4) The simultaneous O^- formation and $\text{Nb}_{\text{Li}}^{4+}:\text{Nb}_{\text{Nb}}^{4+}$ gating are verified within the same sample and are clearly separated in the blue spectral range. Thus, the accepted model of formation, transport and recombination of small bound electron and hole polarons in lithium niobate^{6,8,13–15} is confirmed, in agreement with the state-of-the-art microscopic description of the Nb_{Li} antisite.¹⁶ (5) Similar separation effects may be expected in related systems where the effective charge transport length l_{eff} is smaller than the length scale of the spatial inhomogeneity determining the trap density. This includes, e.g., dielectric oxides periodically poled or with a spatial inhomogeneity of stoichiometry obtained as a consequence of growth striations, doping or any other treatment. Concerning l_{eff} , our experimental study allows to deduce the effective polaron transport length¹⁰ of $l_{\text{eff}} \ll 12 \mu\text{m}$ for the present case of PPLN:Y. (6) The results support the interpretation of the stretched exponential decay arising from the superposition of a multitude of slightly different decay components related to regions with specific defect structure in bulk crystals.

ACKNOWLEDGMENTS

We thank G. Cornelsen, W. Geisler, and R. S. Hardt for experimental and the DFG (Grant Nos. IM 37/5-1 and GRK 695), DAAD (Grant No. 50445542) and OTKA (Grant Nos. K60086 and T047265) for financial support.

*mimlau@uos.de

¹H. Mabuchi, E. S. Polzik, and H. J. Kimble, *J. Opt. Soc. Am. B* **11**, 2023 (1994).

²S. Torbrügge, M. Imlau, B. Schoke, C. Merschjann, O. F. Schirmer, S. Vernay, A. Gross, V. Wesemann, and D. Rytz, *Phys. Rev. B* **78**, 125112 (2008).

³Y. Furukawa, K. Kitamura, A. Alexandrovski, R. K. Route, and M. M. Fejer, *Appl. Phys. Lett.* **78**, 1970 (2001).

⁴D. Berben, K. Buse, S. Wevering, P. Herth, M. Imlau, and T. Woike, *J. Appl. Phys.* **87**, 1034 (2000).

⁵N. F. Evlanova, I. I. Naumova, T. O. Chaplina, S. V. Lavrishchev, and S. A. Blokhin, *Phys. Solid State* **42**, 1727 (2000).

⁶O. F. Schirmer, M. Imlau, C. Merschjann, and B. Schoke, *J. Phys.: Condens. Matter* **21**, 123201 (2009).

⁷O. F. Schirmer, *J. Phys.: Condens. Matter* **18**, R667 (2006).

⁸C. Merschjann, B. Schoke, and M. Imlau, *Phys. Rev. B* **76**,

085114 (2007).

⁹P. Herth, T. Granzow, D. Schaniel, T. Woike, M. Imlau, and E. Krätzig, *Phys. Rev. Lett.* **95**, 067404 (2005).

¹⁰J. Carnicero, M. Carrascosa, G. García, and F. Agulló-López, *Phys. Rev. B* **72**, 245108 (2005).

¹¹B. Sturman, E. Podivilov, and M. Gorkunov, *Phys. Rev. Lett.* **91**, 176602 (2003).

¹²P. Herth, D. Schaniel, T. Woike, T. Granzow, M. Imlau, and E. Krätzig, *Phys. Rev. B* **71**, 125128 (2005).

¹³D. Conradi, C. Merschjann, B. Schoke, M. Imlau, G. Corradi, and K. Polgár, *Phys. Status Solidi (RRL)* **2**, 284 (2008).

¹⁴C. Merschjann, B. Schoke, D. Conradi, M. Imlau, G. Corradi, and K. Polgár, *J. Phys.: Condens. Matter* **21**, 015906 (2009).

¹⁵C. Merschjann, D. Berben, M. Imlau, and M. Wöhlecke, *Phys. Rev. Lett.* **96**, 186404 (2006).

¹⁶H. H. Nahm and C. H. Park, *Phys. Rev. B* **78**, 184108 (2008).